



The following Communications have been judged by at least two referees to be “very important papers” and will be published online at [www.angewandte.org](http://www.angewandte.org) soon:

T. Lewis, M. Faubel, B. Winter, J. C. Hemminger\*  
CO<sub>2</sub> Capture in an Aqueous Solution of an Amine: Role of the Solution Interface

Y. H. Kim, S. Banta\*  
Complete Oxidation of Methanol in an Enzymatic Biofuel Cell by a Self-Assembling Hydrogel Created from Three Modified Dehydrogenases

## Editorial



Theoretical Chemistry—Quo Vadis?

W. Thiel ————— 9216–9217



*“I like refereeing because it gives me a more original picture of the paper.  
The greatest scientific advance in the next decade will be the transition to sustainable and biobased chemistry ...”*  
This and more about Jürgen O. Metzger can be found on page 9237.

## Author Profile

Jürgen O. Metzger ————— 9237

## News



C. Amatore



B. L. Feringa



P. Göllitz



G. J. Hutchings

New Members Elected to the Academy of Europe ————— 9238–9239



J. A. Lercher



M. Orrit



M. Verdaguer



B. M. Weckhuysen

## Books

On Being

Peter Atkins

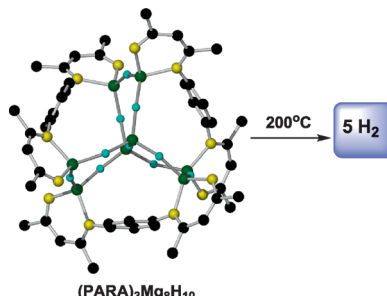
reviewed by U. Meierhenrich — 9240

## Highlights

### Hydrogen Storage

E. Hevia, R. E. Mulvey\* — 9242–9243

A Record-Breaking Magnesium Hydride Molecular Cluster: Implications for Hydrogen Storage

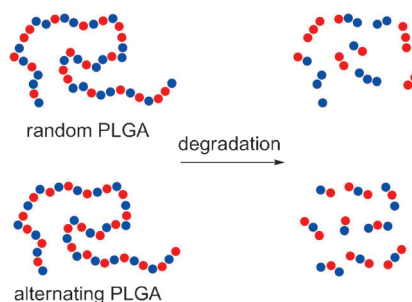


**Hydride carrier:** Making significant progress on the road towards practical hydrogen storage materials for mobile applications, inorganic chemistry shows us how to build the largest ligand-supported magnesium hydride cluster known to date (see picture).

### Polymer Sequences

C. M. Thomas\*, J.-F. Lutz\* — 9244–9246

Precision Synthesis of Biodegradable Polymers



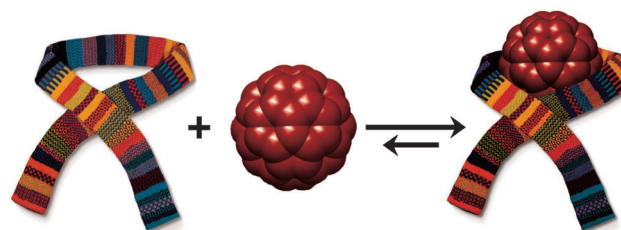
**It's all in the sequence:** The primary structure of poly(lactic-co-glycolic acid) (PLGA), a member of the most widely used class of biodegradable polymers employed in biomedical applications, is demonstrated to strongly influence its degradation properties. Experimental studies evidenced the beneficial effect of ordered monomer sequences on the material properties (see picture).

## Minireviews

### Fullerene Receptors

D. Canevet, E. M. Pérez,  
N. Martín\* — 9248–9259

Wraparound Hosts for Fullerenes: Tailored Macrocycles and Cages



**All wrapped up:** In the field of fullerene recognition, chemists are currently facing new challenges dealing with the selective extraction of higher fullerenes, their chiral resolution, or their organization in

molecular materials. In this regard, the new generation of macrocyclic hosts looks particularly promising and has already allowed important breakthroughs.

**For the USA and Canada:**  
ANGEWANDTE CHEMIE International Edition (ISSN 1433-7851) is published weekly by Wiley-VCH, PO Box 191161, 69451 Weinheim, Germany. Air freight and mailing in the USA by Publications Expediting Inc., 200 Meacham Ave., Elmont, NY 11003. Periodicals

postage paid at Jamaica, NY 11431. US POSTMASTER: send address changes to *Angewandte Chemie*, Journal Customer Services, John Wiley & Sons Inc., 350 Main St., Malden, MA 02148-5020. Annual subscription price for institutions: US\$ 11,738/10,206 (valid for print and electronic / print or electronic delivery); for

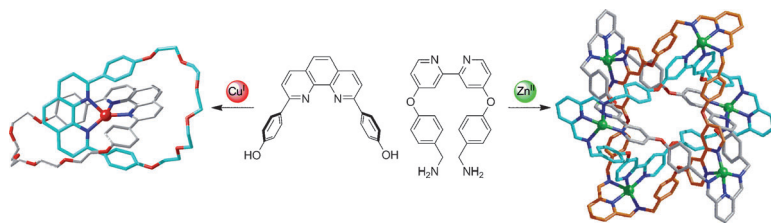
individuals who are personal members of a national chemical society prices are available on request. Postage and handling charges included. All prices are subject to local VAT/sales tax.

## Reviews

### Interlocked Molecules

J. E. Beves, B. A. Blight, C. J. Campbell,  
 D. A. Leigh,\*  
 R. T. McBurney ————— 9260–9327

Strategies and Tactics for the Metal-Directed Synthesis of Rotaxanes, Knots, Catenanes, and Higher Order Links



**Knots and crossings:** Metal ions have been employed in diverse ways in the assembly of mechanically interlocked architectures (see scheme). The range of

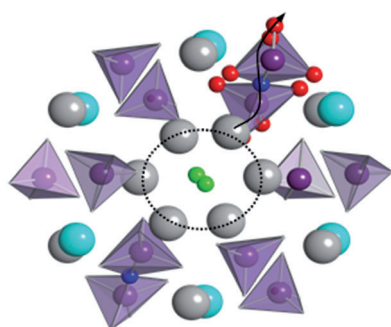
product topologies spans from catenanes and rotaxanes to trefoil knots, Solomon links, and Borromean rings.

## Communications

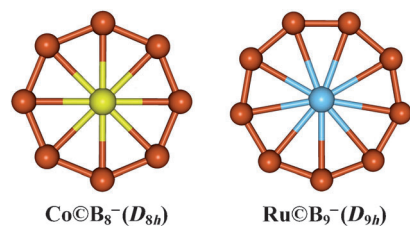
### Fuel Cells

P. M. Panchmatia, A. Orera, G. J. Rees,  
 M. E. Smith, J. V. Hanna,\* P. R. Slater,\*  
 M. S. Islam\* ————— 9328–9333

Oxygen Defects and Novel Transport Mechanisms in Apatite Ionic Conductors: Combined  $^{17}\text{O}$  NMR and Modeling Studies



**Germanium-based apatite** compounds are fast oxide-ion conductors for potential use in fuel cells. A combination of solid-state  $^{17}\text{O}$  NMR spectroscopy, atomistic modeling, and DFT techniques help to elucidate oxygen defect sites and novel cooperative mechanisms of ion conduction. The picture shows oxygen diffusion in the studied apatite compound from molecular dynamics simulations.



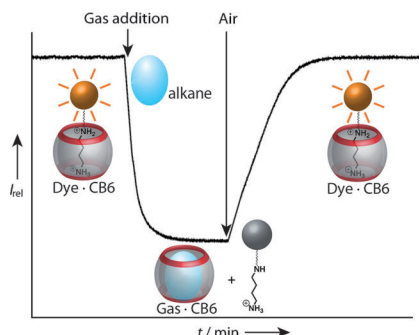
**Perfect symmetry:** Photoelectron spectroscopy and theoretical calculations show that the  $\text{B}_8$  and  $\text{B}_9$  rings are stabilized by the metal atoms in  $\text{Co}@\text{B}_8^-$  and  $\text{Ru}@\text{B}_9^-$ , which possess  $D_{8h}$  and  $D_{9h}$  symmetry, respectively (see picture). The bonding between the metal atom and the boron ring is described by six delocalized  $\sigma$  electrons and six delocalized  $\pi$  electrons, which result in double aromaticity.

### Aromaticity

C. Romanescu, T. R. Galeev, W. L. Li,  
 A. I. Boldyrev,\* L. S. Wang\* 9334–9337

Aromatic Metal-Centered Monocyclic Boron Rings:  $\text{Co}@\text{B}_8^-$  and  $\text{Ru}@\text{B}_9^-$

**Hydrocarbons** are no longer afraid of water when they are reversibly encapsulated by cucurbituril (see picture). The pumpkin-shaped molecular container displays a high affinity and selectivity towards neutral molecules in salt-free aqueous solutions. A supramolecular sensing ensemble, composed of cucurbit[6]uril and an anchored indicator dye, is introduced as a highly sensitive fluorescence-based online detection tool for gas binding in solution.



### Supramolecular Chemistry

M. Florea, W. M. Nau\* — 9338–9342

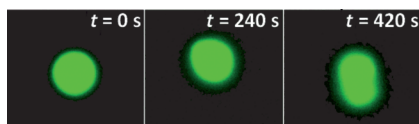
Strong Binding of Hydrocarbons to Cucurbituril Probed by Fluorescent Dye Displacement: A Supramolecular Gas-Sensing Ensemble

## Artificial Cells

R. Krishna Kumar, X. Yu, A. J. Patil, M. Li, S. Mann\* — 9343–9347



Cytoskeletal-like Supramolecular Assembly and Nanoparticle-Based Motors in a Model Protocell



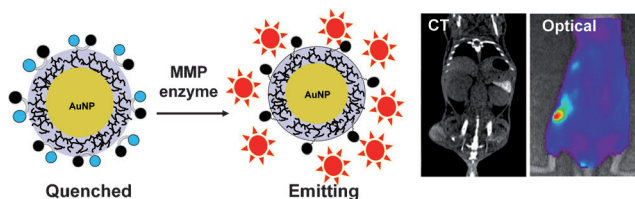
**Busting a move:** Enzyme-mediated assembly of an amino acid derived supramolecular hydrogel is used to produce a vesicle-based protocell model with a primitive cytoskeletal-like interior. The vesicles show temperature-induced changes in morphology (see picture), and undergo chemically driven self-propulsion when Pt nanoparticles are attached to their external surface and  $\text{H}_2\text{O}_2$  is added to the solution.

## Imaging Agents

I. C. Sun, D. K. Eun, H. Koo, C. Y. Ko, H. S. Kim, D. K. Yi, K. Choi, I. C. Kwon, K. Kim,\* C. H. Ahn\* — 9348–9351



Tumor-Targeting Gold Particles for Dual Computed Tomography/Optical Cancer Imaging



**Double spotlight:** A dual imaging probe with gold nanoparticles (AuNPs) for computed tomography (CT) and optical imaging exhibits have been developed (see picture). The excellent stability, tumor targeting ability, enhanced X-ray

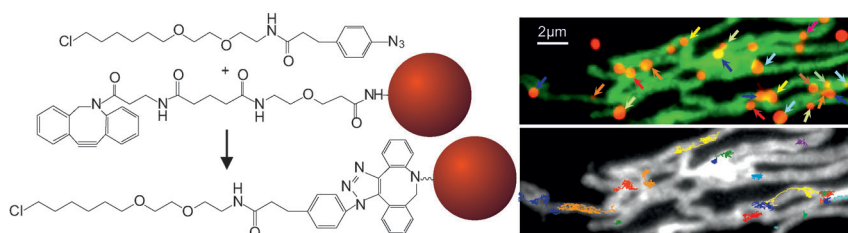
absorption, and matrix metalloproteinase (MMP) activatable fluorescence recovery was achieved by surface modification of AuNPs with glycol chitosan and fluorescent MMP peptide probes.

## Nanoparticles in Biology

D. Liße, V. Wilkens, C. You, K. Busch, J. Piehler\* — 9352–9355



Selective Targeting of Fluorescent Nanoparticles to Proteins Inside Live Cells



**Tracking single proteins in cells:** An optimized substrate based on a click reaction was designed for specific, irreversible targeting of nanoparticles to proteins fused to an engineered halo-

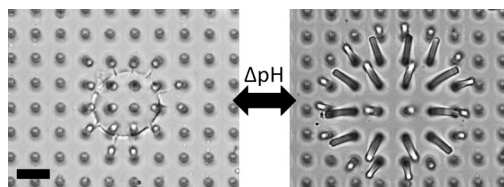
alkane dehalogenase (HaloTag) in the cytoplasm of live cells. Thus, proteins in the membrane of mitochondria could be tracked over extended times and with nanometer resolution (see picture).

## Hydrogels

L. D. Zarzar, P. Kim, M. Kolle, C. J. Brinker, J. Aizenberg,\* B. Kaehr\* — 9356–9360



Direct Writing and Actuation of Three-Dimensionally Patterned Hydrogel Pads on Micropillar Supports

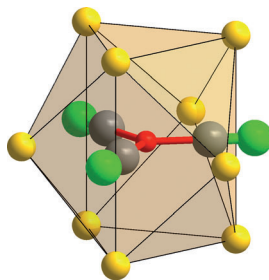


**Written response:** Freely swelling, three-dimensionally patterned responsive hydrogels fabricated by multiphoton lithography on the tips of flexible pillars provide unique capabilities for the design of adaptive systems. The resulting mate-

rials have tunable actuation direction and angle, sensitive optical response, and precise spatial integration of gels with varying pH and temperature response (see picture; scale bar: 20 μm).



**More than meets the eye:** The trigonal-planar complex  $[\text{Co}(\text{CN})_3]^{6-}$  (see structure, Co red, C gray, N green; alkaline-earth-metal counterions are yellow) has some surprises in store. The CN ligand displays variation in bond length and charge, and Co follows a closed-shell ( $d^{10}$ ) concept.



## Metalates

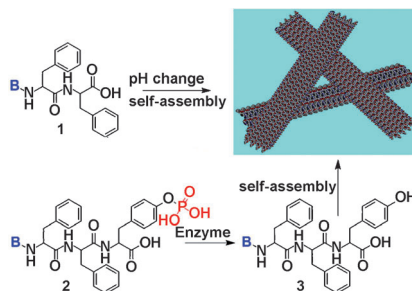


P. Höhn,\* F. Jach, B. Karabiyik, Y. Prots, S. Agrestini, F. R. Wagner, M. Ruck, L. H. Tjeng, R. Kniep\* — 9361–9364

$\text{Sr}_3[\text{Co}(\text{CN})_3]$  and  $\text{Ba}_3[\text{Co}(\text{CN})_3]$ : Crystal Structure, Chemical Bonding, and Conceptual Considerations of Highly Reduced Metalates



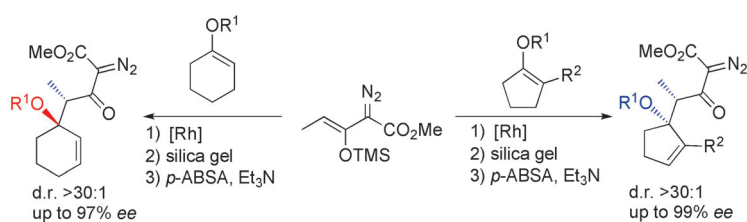
**Watson–Crick interactions:** The conjugation of nucleobases (B = thymine, adenine, cytosine, and guanine; see picture) with small peptides affords a novel kind of supramolecular nanofibers and hydrogels, which exhibit a high biocompatibility and biostability and are regarded as promising new biomaterials.



## Supramolecular Hydrogels

X. M. Li, Y. Kuang, H.-C. Lin, Y. Gao, J. F. Shi, B. Xu\* — 9365–9369

Supramolecular Nanofibers and Hydrogels of Nucleopeptides



## C–H Functionalization

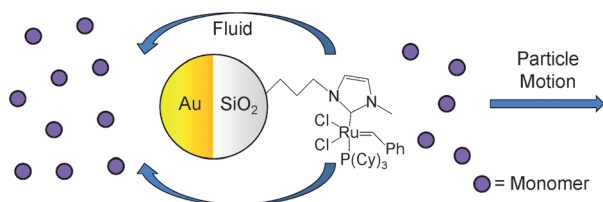
Y. Lian, K. I. Hardcastle, H. M. L. Davies\* — 9370–9373

Computationally Guided Stereocontrol of the Combined C–H Functionalization/Cope Rearrangement



**Diastereoselectivity in control:** The synthetic utility of the C–H functionalization/Cope rearrangement reaction has been greatly expanded by the design of substrates that will react through a boat

transition state instead of a chair transition state. The products are formed with the opposite diastereoselectivity as previously obtained (see scheme, ABSA = acetamidobenzenesulfonylazide).



## Micromotors

R. A. Pavlick, S. Sengupta, T. McFadden, H. Zhang, A. Sen\* — 9374–9377

A Polymerization-Powered Motor



**Polymer powered!** A polymerization reaction has been used to power the first micromotor outside biological systems. The motor employs a form of Grubbs' catalyst asymmetrically bound to gold–

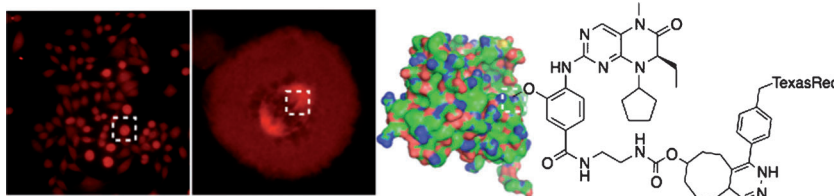
silica Janus microspheres (see picture). These motors show increased diffusion of up to 70% when placed in solutions of the monomer. The motors also exhibit chemotaxis when placed in a monomer gradient.

## Live Cell Imaging

G. Budin, K. S. Yang, T. Reiner,  
R. Weissleder\* 9378–9381



Bioorthogonal Probes for Polo-like  
Kinase 1 Imaging and Quantification



**Click inside:** A nuclear protein target, polo-like kinase 1 (PLK1) was imaged using a biocompatible bioorthogonal ligation between a specific drug and a fluorescent dye in live cells (see picture). Colocalization of the dye and the protein

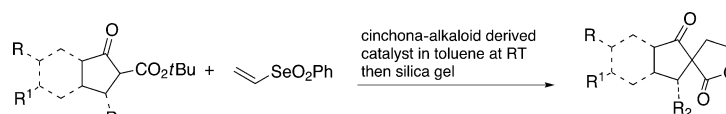
target was confirmed by antibody staining and by expressing a GFP construct of PLK1. The two-step PLK1 imaging procedure was used to quantify PLK1 expression levels in cancer cell lines of various tissue origins.

## Organocatalysis

S. Sternativo, A. Calandriello,  
F. Costantino, L. Testaferri, M. Tiecco,  
F. Marini\* 9382–9385



A Highly Enantioselective One-Pot  
Synthesis of Spirolactones by an  
Organocatalyzed Michael Addition/  
Cyclization Sequence



**Spiroing in control:** A novel organocatalytic Michael addition/cyclization sequence based on the bis(electrophilic) properties of vinyl selenones has been successfully employed for the synthesis of densely functionalized spirocyclic com-

pounds (see scheme). By using a simple one-pot procedure and mild reaction conditions, spirocyclic compounds were synthesized in high yields and with high levels of enantioselectivity (90–98% *ee*).

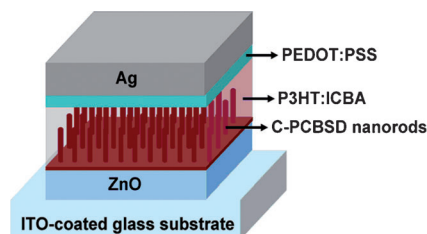


## Organic Solar Cells

C.-Y. Chang, C.-E. Wu, S.-Y. Chen, C. Cui,  
Y.-J. Cheng, C.-S. Hsu,\* Y.-L. Wang,\*  
Y. Li 9386–9390



Enhanced Performance and Stability of a  
Polymer Solar Cell by Incorporation of  
Vertically Aligned, Cross-Linked Fullerene  
Nanorods



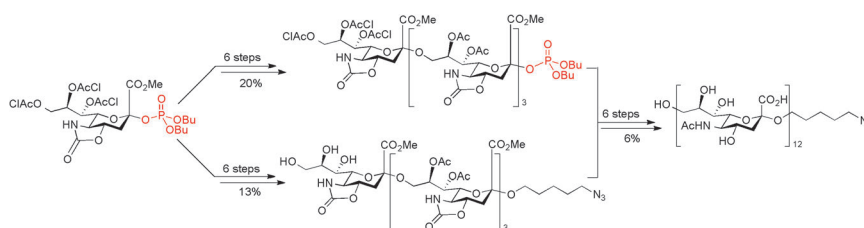
**Let the sun shine in:** Highly efficient and stable polymer bulk-heterojunction solar cells can be achieved by the incorporation of vertically oriented, cross-linked polymer nanorods (see picture). The device exhibits a record power conversion efficiency of 7.3%.

## Oligosaccharides

K.-C. Chu, C.-T. Ren, C.-P. Lu, C.-H. Hsu,  
T.-H. Sun, J.-L. Han, B. Pal, T.-A. Chao,  
Y.-F. Lin, S.-H. Wu, C.-H. Wong,\*  
C.-Y. Wu\* 9391–9395



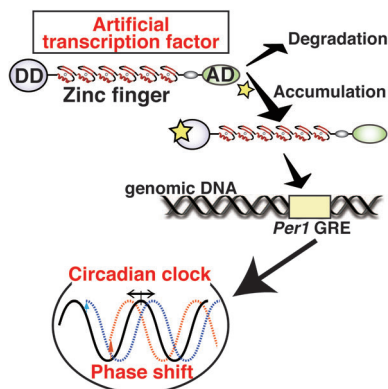
Efficient and Stereoselective Synthesis of  
 $\alpha(2\rightarrow9)$  Oligosialic Acids: From  
Monomers to Dodecamers



**The chain gang:** The  $\alpha(2\rightarrow9)$  dodeciasialic acid has been stereoselectively synthesized in 12 steps by using a convergent block synthesis (see scheme). The use of chloroacetyl protecting groups and a

phosphate group as a leaving group led to the improvement of the  $\alpha$  selectivity of the glycosylation reactions, thus allowing synthesis of oligomers.

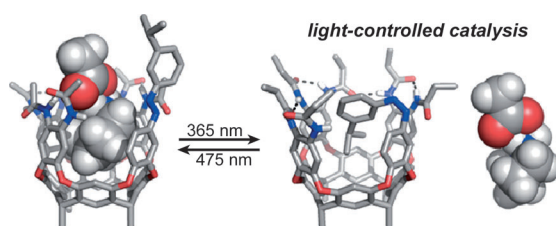
**I got rhythm:** The circadian clock is driven by transcription–translation feedback loops. The circadian time can be altered by creating an artificial zinc finger protein specifically binding to the glucocorticoid responsive element (GRE) on the *Period1* promoter (see picture; DD = destabilizing domain, AD = activation domain). This artificial protein directly controls the clock machinery.



### Circadian Rhythm

M. Imanishi,\* A. Nakamura, M. Doi, S. Futaki, H. Okamura\* — **9396–9399**

Control of Circadian Phase by an Artificial Zinc Finger Transcription Regulator



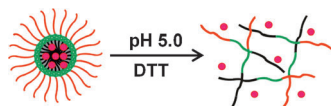
**Catalytic guest stars:** A cavitand with an azobenzene wall adopts an introverted shape when irradiated with UV light. This conformation has been characterized in solution and the solid state and is used to

control guest binding. By incorporating an organocatalyst guest, the rate of the Knoevenagel condensation is controlled with light.

### Supramolecular Catalysis

O. B. Berryman, A. C. Sather, A. Lledó, J. Rebek, Jr.\* — **9400–9403**

Switchable Catalysis with a Light-Responsive Cavitand



**On the double:** A highly packed interlayer-crosslinked micelle (HP-ICM) with pH and reduction sensitivity was developed for targeted drug release (see picture; DTT = dithiothreitol, red circles = doxorubicin). The HP-ICM suppresses drug leakage in blood circulation while rapidly releasing drug inside lysosomes of cancer cells. Biological studies revealed the potential of the dual-sensitive HP-ICM in cancer treatment.

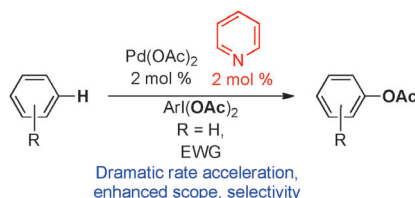
### Drug Delivery

J. Dai, S. Lin, D. Cheng, S. Zou, X. Shuai\* — **9404–9408**

Interlayer-Crosslinked Micelle with Partially Hydrated Core Showing Reduction and pH Dual Sensitivity for Pinpointed Intracellular Drug Release



**Less is more:** The rational optimization and general applicability of the catalytic system  $\text{Pd}(\text{OAc})_2/\text{pyridine}$  is described (see scheme). The catalyst shows excellent reactivity in the C–H oxygenation of simple aromatic substrates. The Pd/pyridine ratio is critical as the use of one equivalent of pyridine per Pd center leads to dramatic enhancements in both reactivity and site selectivity in comparison to  $\text{Pd}(\text{OAc})_2$  alone.



### C–H Activation

M. H. Emmert, A. K. Cook, Y. J. Xie, M. S. Sanford\* — **9409–9412**

Remarkably High Reactivity of  $\text{Pd}(\text{OAc})_2/\text{Pyridine}$  Catalysts: Nondirected C–H Oxygenation of Arenes

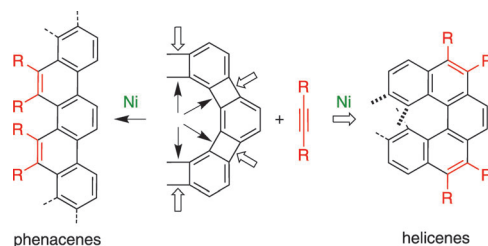


## Polycyclic Aromatics

Z. Gu, G. B. Boursalian, V. Gandon,  
R. Padilla, H. Shen, T. V. Timofeeva,  
P. Tongwa, K. P. C. Vollhardt,\*  
A. A. Yakovenko — 9413–9417



Activated Phenacenes from Phenylenes by  
Nickel-Catalyzed Alkyne Cycloadditions



**Going zigzag, helical, or in-between:**  
Angular phenylenes show a propensity for  
adding alkynes from the bay region in  
processes catalyzed by  $[\text{Ni}(\text{cod})(\text{PMe}_3)_2]$   
(see scheme). These transformations

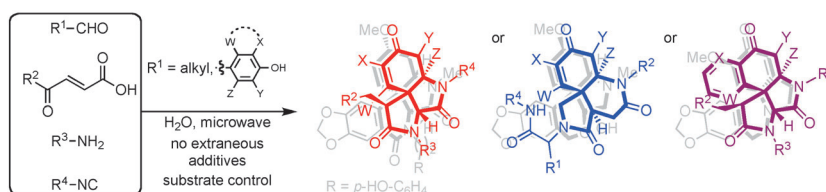
generate novel strain- and electronically  
activated phenacenes. Mechanistic stud-  
ies in conjunction with DFT calculations  
( $\text{R} = \text{Ph}$ ) provide a plausible mechanistic  
picture.

## Multicomponent Reactions

S. Santra, P. R. Andreana\* — 9418–9422



A Bioinspired Ugi/Michael/Aza-Michael  
Cascade Reaction in Aqueous Media:  
Natural-Product-like Molecular Diversity



**Whole in one!** A one-pot microwave-  
assisted reaction sequence that consists  
of an Ugi/Michael/aza-Michael trans-  
formation gives access to quaternary spiro-  
centers leading to *Amaryllidaceae* and  
*Erythrina* alkaloid like compounds (see

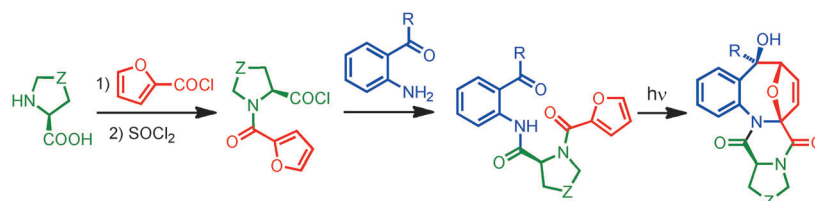
scheme). The process produces four  
stereogenic centers and six contiguous  
bonds, and provides products with good  
to excellent yields and appreciable dia-  
stereoselectivity.

## Photochemistry

O. A. Mukhina, N. N. Bhuvan Kumar,  
T. M. Arisco, R. A. Valiulin, G. A. Metzel,  
A. G. Kutateladze\* — 9423–9428



Rapid Photoassisted Access to N,O,S-  
Polyheterocycles with Benzoazocine and  
Hydroquinoline Cores: Intramolecular  
Cycloadditions of Photogenerated  
Azaxylylenes



**Ring the changes:** A new photoassisted  
approach to give conformationally con-  
strained N,O,S-polyheterocyclic scaffolds  
of unprecedented topologies was  
achieved by intramolecular [4 + 4] and  
[4 + 2] cycloadditions of photogenerated

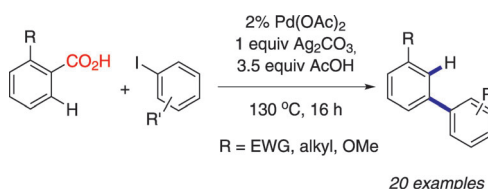
*o*-azaxylylenes (23 examples; see  
scheme). The precursors can be readily  
assembled by simple and high-yielding  
reactions, thus making this a powerful  
synthetic method amenable to high-  
throughput diversity-oriented synthesis.

## C–H Arylation

J. Cornella, M. Righi,  
I. Larrosa\* — 9429–9432



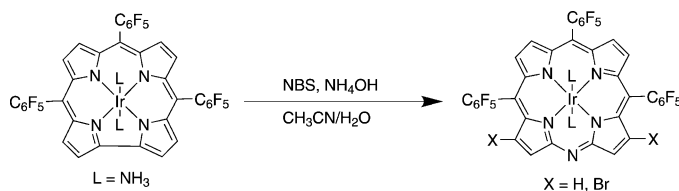
Carboxylic Acids as Traceless Directing  
Groups for Formal *meta*-Selective Direct  
Arylation



**Without a trace:** The first *meta*-selective  
direct C–H arylation that uses iodoarenes  
as coupling partners is reported (see  
scheme, EWG = electron-withdrawing  
group). This process utilizes carboxylic

acid units as temporary directing groups  
that are cleaved during the reaction,  
leaving no trace in the resulting biaryl  
products.





**A new route to rare porphyrinoids:** The non-innocence of the corrole ring allows the oxidative ring insertion of a nitrogen atom under mild conditions (see scheme; NBS = *N*-bromosuccinimide). The resulting *meso*-substituted azaporphyrins

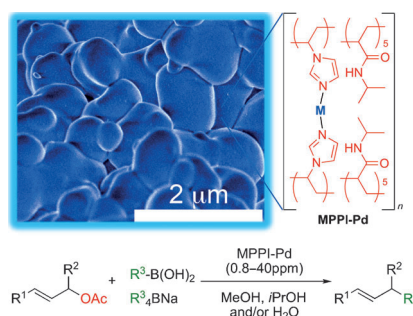
exhibit high-energy Soret absorption bands and red luminescence. This new synthetic route will allow for the development of novel azaporphyrin complexes with relevance to the study of biomimetic oxidations.

### Corrole Expansion

J. H. Palmer,\* T. Brock-Nannestad, A. Mohammed, A. C. Durrell, D. VanderVelde, S. Virgil, Z. Gross, H. B. Gray **9433–9436**

Nitrogen Insertion into a Corrole Ring: Iridium Monoazaporphyrins

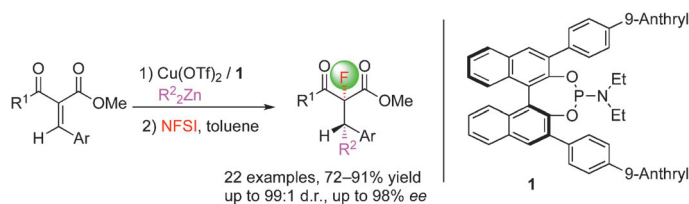
**Gobs of globules:** A polymeric imidazole/acrylamide palladium catalyst, MPPI-Pd ( $M = \text{Pd}^{\text{II}}\text{Cl}$  and  $\text{Pd}^0$ ), was utilized for the allylic arylation/alkenylation of allylic esters with aryl/alkenylboronic acids and tetraaryl borates. Low catalyst loadings efficiently promoted the reaction with a catalytic turnover number of 20 000–1 250 000. The catalyst can be reused without loss of catalytic activity.



### Supramolecular Catalysts

S. M. Sarkar, Y. Uozumi,\* Y. M. A. Yamada\* **9437–9441**

A Highly Active and Reusable Self-Assembled Poly(Imidazole/Palladium) Catalyst: Allylic Arylation/Alkenylation



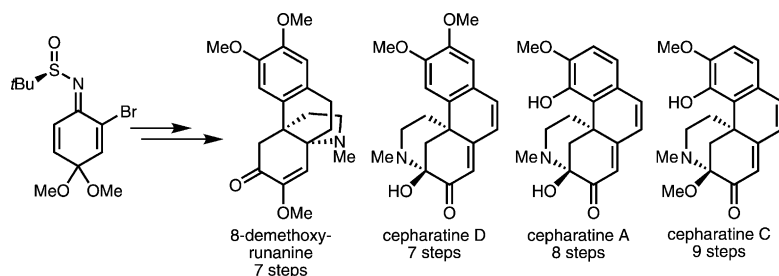
**Long arm of the law:** The long-armed phosphoramidite **1** was used as a catalyst for the title reaction of acyclic alkylidene  $\beta$ -ketoesters with dialkylzinc and fluorinating reagents. The products, containing

adjacent carbon- and fluorine-substituted stereocenters, are obtained in high yield as well as diastereo- and enantioselectivity. NFSI = *N*-fluorobenzenesulfonimide.

### Asymmetric Catalysis

L. Wang, W. Meng, C.-L. Zhu, Y. Zheng, J. Nie, J.-A. Ma\* **9442–9446**

The Long-Arm Effect: Influence of Axially Chiral Phosphoramidite Ligands on the Diastereo- and Enantioselectivity of the Tandem 1,4-Addition/Fluorination



**All together!** A unified synthetic strategy has resulted in the first enantioselective total syntheses of the natural products 8-

demethoxyrunanine and cepharatines A, C, and D.

### Natural Product Synthesis

K. V. Chuang, R. Navarro, S. E. Reisman\* **9447–9451**

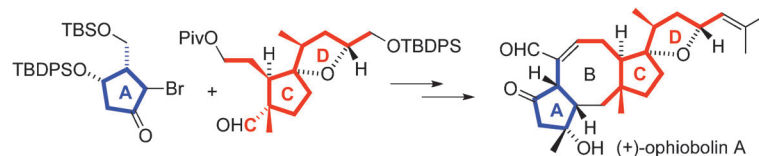
Short, Enantioselective Total Syntheses of (–)-8-Demethoxyrunanine and (–)-Cepharatines A, C, and D

## Natural Product Synthesis

K. Tsuna, N. Noguchi,  
M. Nakada\* 9452–9455



Convergent Total Synthesis of  
(+)-Ophiobolin A



**At long last:** The enantioselective total synthesis of the title compound, which was isolated in 1958, proceeds by a convergent approach. The assembly of the C,D-ring fragment and the A-ring frag-

ment of the core structure is achieved by employing a Reformatsky-type reaction. The eight-membered carbocyclic B ring is efficiently constructed by a challenging ring-closing metathesis (see scheme).

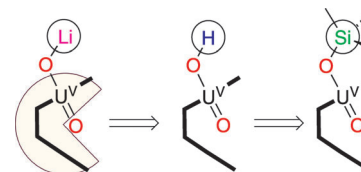
## Uranyl Reactivity

P. L. Arnold,\* A.-F. Pécharman,  
J. B. Love\* 9456–9458



Oxo Group Protonation and Silylation of  
Pentavalent Uranyl Pacman Complexes

**New bonds for the uranyl:** The controlled conversion of an uranyl oxo group ( $[\text{UO}_2]^+$ ) into covalently bonded  $\text{UO}-\text{H}$  and  $\text{UO}-\text{Si}$  groups is described for pentavalent uranyl Pacman complexes. The unusual oxo-hydroxy motif is achieved by a protonation reaction and retains the normally unstable  $\text{U}^{\text{V}}$  uranyl oxidation state. This product is readily silylated by treatment with a chlorosilane resulting in  $\text{UO}-\text{Si}$  bond formation (see scheme).



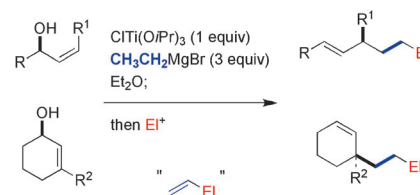
## Alkylation

P. P. Das, I. L. Lysenko,  
J. K. Cha\* 9459–9461



Stereoselective Alkylation of Allylic  
Alcohols: Tandem Ethylation and  
Functionalization

**A versatile** formal  $\text{S}_{\text{N}}2'$  alkylation of allylic alcohols has been devised by means of the Kulinkovich reagent and in situ elaboration of the presumed alkyltitanium intermediates with electrophiles (see scheme). The utility of this method has been demonstrated in the stereoselective construction of all-carbon quaternary centers.

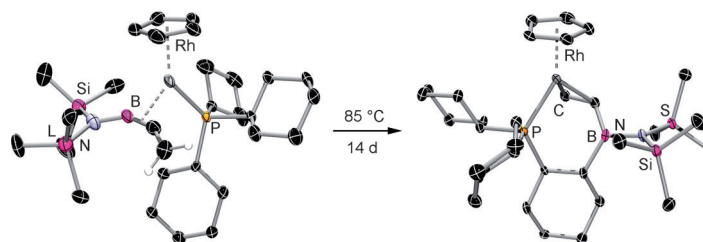


## Boracumulene Complexes

H. Braunschweig,\* Q. Ye, A. Damme,  
T. Kupfer, K. Radacki, J. Wolf 9462–9466



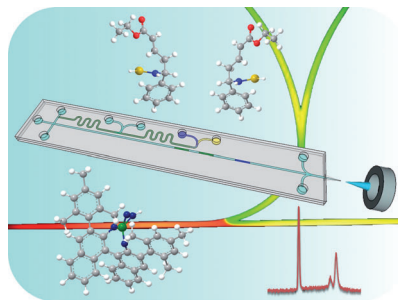
Synthesis of 1-Aza-2-borabutatriene  
Rhodium Complexes by Thermal Borylene  
Transfer from  $[(\text{OC})_5\text{Mo}=\text{BN}(\text{SiMe}_3)_2]$



**Borylene on me:** An unprecedented borylene transfer to metal-carbon double bonds afforded the title compounds. Preliminary studies revealed a thermally induced change of coordination mode from  $\text{B}-\text{C}$  to  $\text{C}-\text{C}$  and subsequent highly

stereoselective  $\text{C}-\text{H}$  activation by the  $\text{B}=\text{C}$  bond.  $[(\eta^5-\text{C}_5\text{H}_5)\text{Rh}(\text{PCy}_3)\{(\text{B},\text{C}-\eta^2)-(\text{SiMe}_3)_2\text{N}=\text{B}=\text{C}=\text{CH}_2\}]$  and its rearrangement product were both characterized by X-ray crystallography (see picture).

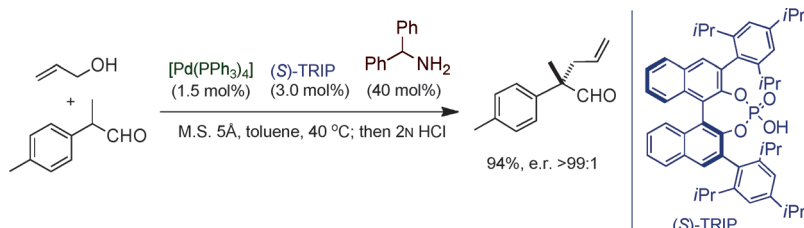
**Organocatalysis meets chip MS:** By integrating asymmetric organocatalysis and analysis on a chip (see picture), optimization of reactions can be achieved with minimal consumption of resources in a short period of time.



### Lab on a Chip

S. Fritzsche, S. Ohla, P. Glaser, D. S. Giera, M. Sickert, C. Schneider, D. Belder\* — 9467 – 9470

Asymmetric Organocatalysis and Analysis on a Single Microfluidic Nanospray Chip



### Triple Catalysis

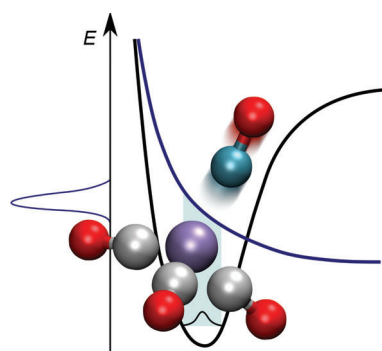
G. Jiang, B. List\* — 9471 – 9474

Direct Asymmetric  $\alpha$ -Allylation of Aldehydes with Simple Allylic Alcohols Enabled by the Concerted Action of Three Different Catalysts



**Triple catalysis:** The title reaction between  $\alpha$ -branched aldehydes and allylic alcohols, which generates all-carbon quaternary stereogenic centers, constitutes the first asymmetric Tsuji–Trost-type  $\alpha$ -allylation

of carbonyl compounds with allylic alcohols (see scheme). This reaction is catalyzed by three different species,  $[\text{Pd}(\text{PPh}_3)_4]$ , the chiral Brønsted acid TRIP, and benzhydryl amine.

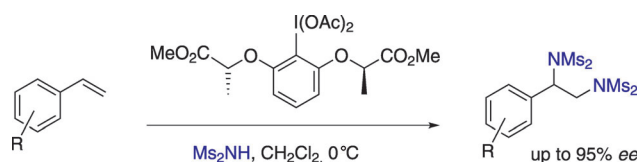


**Put a number on it:** Absolute cross-sections for dissociative electron attachment (DEA) to the common precursor molecule cobalt tricarbonyl nitrosyl in the gas phase are reported (see scheme, Co dark blue, O red, C gray, N light blue) along with the branching ratios for the negative ions and the electron affinities for the neutral radical fragments. Further, a general mechanism of DEA is proposed for metal–carbonyl compounds.

### Gas-Phase Chemistry

S. Engmann, M. Stano, Š. Matejčík,\* O. Ingólfsson\* — 9475 – 9477

The Role of Dissociative Electron Attachment in Focused Electron Beam Induced Processing: A Case Study on Cobalt Tricarbonyl Nitrosyl



### Asymmetric Synthesis

C. Röben, J. A. Souto, Y. González, A. Lishchynskiy, K. Muñiz\* — 9478 – 9482

Enantioselective Metal-Free Diamination of Styrenes

**Metal-free and asymmetric:** The first enantioselective diamination of styrenes simply requires a chiral hypervalent iodine(III) reagent as an oxidant and

bismesylimide as a nitrogen source (see scheme, Ms = methanesulfonyl). The reaction proceeds under mild conditions and with high enantiomeric excess.

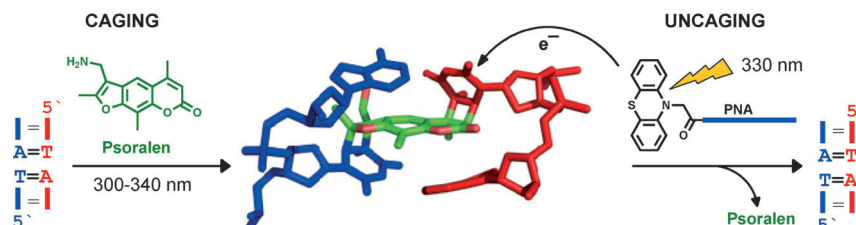


## DNA Repair

T. Stafforst,\* D. Hilvert\* — 9483–9486



Photolyase-like Repair of Psoralen-Crosslinked Nucleic Acids



**Psoralen-derived photolesions** are efficiently repaired by a photolyase-like mechanism. The removal of the inter-strand crosslink by photoelectron injection confers control over biochemical

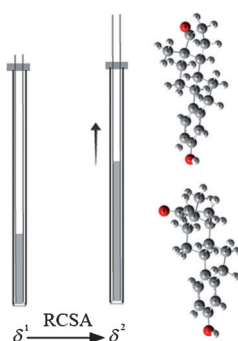
processes by light (see picture). This paves the way to new, site-selective uncaging applications, as demonstrated with a primer extension assay.

## Configuration Determination

F. Hallwass, M. Schmidt, H. Sun, A. Mazur, G. Kummerlöwe, B. Luy, A. Navarro-Vázquez, C. Griesinger,\* U. M. Reinscheid\* — 9487–9490



Residual Chemical Shift Anisotropy (RCSA): A Tool for the Analysis of the Configuration of Small Molecules



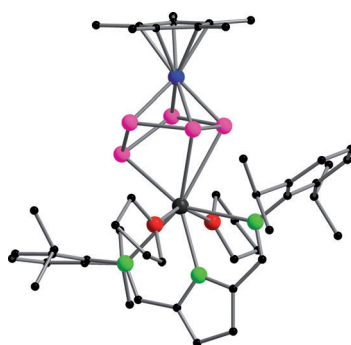
**Together we are strong:** A new, robust method allows the measurement of residual chemical shift anisotropies for the determination of conformation and configuration of molecules in organic solvents. The power of the method is shown by the example of estrone and 13-*epi*-estrone (see structures), where only the combined use of residual chemical shift anisotropies and residual dipolar couplings leads to the distinction of the two diastereomers.

## Polyphosphides

T. Li, J. Wiecko, N. A. Pushkarevsky, M. T. Gamer, R. Köppe, S. N. Konchenko, M. Scheer, P. W. Roesky\* — 9491–9495



Mixed-Metal Lanthanide–Iron Triple-Decker Complexes with a *cyclo*-P<sub>5</sub> Building Block



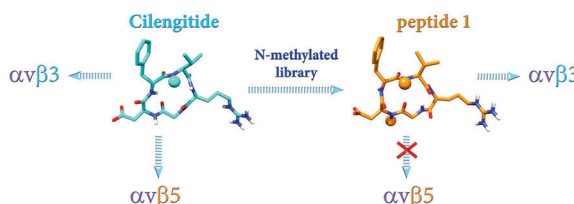
**Triple-decker complexes** with mixed d/f-block metals that have a purely inorganic middle deck were unknown. A mixed-metal iron–samarium complex is presented with a *cyclo*-P<sub>5</sub> polyphosphide between the metal centers (see picture; Sm large black, C small black, Fe blue, N green, O red, P pink). This compound can be obtained as either a monomer or a dimer depending on the reaction conditions.

## Drug Selectivity

C. Mas-Moruno, J. G. Beck, L. Doedens, A. O. Frank, L. Marinelli, S. Cosconati, E. Novellino, H. Kessler\* — 9496–9500

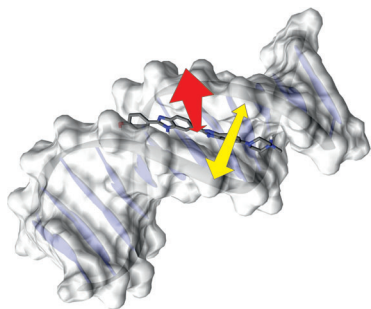


Increasing αvβ3 Selectivity of the Anti-Angiogenic Drug Cilengitide by N-Methylation



**A subtle change:** Structural changes upon amide bond methylation improve the selectivity of the anti-angiogenic drug Cilengitide, which after N-methylation at

distinct positions discriminates between the closely related pro-angiogenic integrins αvβ3 and αvβ5 (see scheme).



**Riding the waves:** In a DNA–ligand complex, the time-dependent Stokes shift shows initial oscillation. Molecular dynamics simulations help assign this ripple to coherent in/out motion of the ligand together with breathing of the minor groove (see picture).

### Femtosecond Spectroscopy

M. Sajadi, K. E. Furse, X.-X. Zhang,  
L. Dehmel, S. A. Kovalenko,  
S. A. Corcelli,\*  
N. P. Ernsting\* \_\_\_\_\_ **9501 – 9505**

Detection of DNA–Ligand Binding  
Oscillations by Stokes-Shift  
Measurements



Supporting information is available  
on [www.angewandte.org](http://www.angewandte.org)  
(see article for access details).



A video clip is available as Supporting  
Information on [www.angewandte.org](http://www.angewandte.org)  
(see article for access details).



This article is available  
online free of charge  
(Open Access)

## Looking for outstanding employees?

Do you need another expert for your excellent team?

... Chemists, PhD Students, Managers, Professors, Sales Representatives...

Place an advert in the printed version and have it made available online for  
1 month, free of charge! Gesellschaft Deutscher Chemiker

**Angewandte Chemie International Edition**

Advertising Sales Department: Marion Schulz

Phone: 0 62 01 - 60 65 65

Fax: 0 62 01 - 60 65 50

E-Mail: [MSchulz@wiley-vch.de](mailto:MSchulz@wiley-vch.de)

## Service

**Spotlight on Angewandte's  
Sister Journals** \_\_\_\_\_ **9234 – 9236**

**Preview** \_\_\_\_\_ **9507**



## Corrigendum

Photoredox Catalysis: A Mild, Operationally Simple Approach to the Synthesis of  $\alpha$ -Trifluoromethyl Carbonyl Compounds

P. V. Pham, D. A. Nagib,  
D. W. C. MacMillan\* — 6119–6122

Angew. Chem. Int. Ed. 2011, 50

DOI 10.1002/anie.201101861

This Communication contains a typesetting mistake. In Table 2, inadvertently the same chemical equation was used as in Table 3. The correct Table 2 is shown below.

**Table 2:** Trifluoromethylation of enolsilanes: ketone scope.

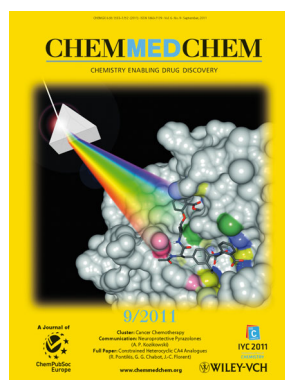
	$\text{CF}_3\text{I}$		$0.5 \text{ mol\% } \mathbf{1} \cdot \text{H}_2\text{O}$	
enolsilane	feedstock reagent	household light	$i\text{Pr}_2\text{EtN}, \text{H}_2\text{O}$ THF, 23 °C	
			$\alpha\text{-CF}_3 \text{ ketone}$	
Entry		Product	Yield <sup>[a]</sup>	
	R =	1: H	92%	4: I 83%
		2: OMe	78%	5: Br 85%
		3: CN	66%	6: Cl 85%
				7: F 80%
		8: 72% <sup>[b]</sup>		
		9: 74% <sup>[c,d]</sup>		
		10: X = O <sup>[e]</sup> 64%		
	11: X = S <sup>[e]</sup> 72%			
	12: R = Boc <sup>[e]</sup> 73%			
	13: R = Cbz <sup>[e]</sup> 59%			
	14: 68% <sup>e</sup>			
	15: 84% <sup>[b]</sup>			
	16: 76%			

[a] Yield of isolated product; SiR<sub>3</sub> = TIPS unless otherwise noted. [b] TES ether employed. [c] TBS ether employed. [d] 2.2:1 d.r. [e] With NaHCO<sub>3</sub> in MeCN and TES ether.

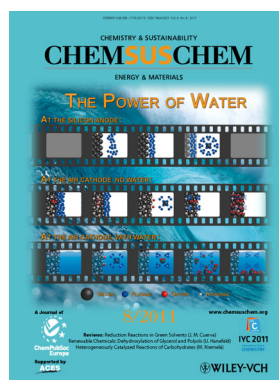
Check out these journals:



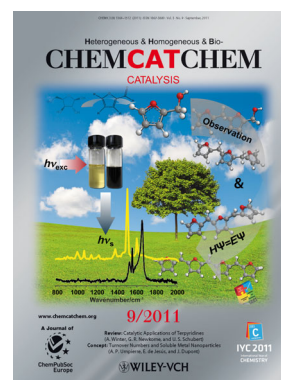
www.chemasianj.org



www.chemmedchem.org



www.chemsuschem.org



www.chemcatchem.org